Electronic Supplementary Material (ESI) for Energy & Environmental Science.
This journal is © The Royal Society of Chemistry 2017

Supporting Information

Electrocatalysis of Polysulfide Conversion by Sulfur-deficient MoS_2 Nanoflakes for Lithium-sulfur Batteries

Haibin Lin[1], Liuqing Yang[1], Xi Jiang[1], Guochun Li[1], Tianran Zhang[1], Qiaofeng Yao[1], Guangyuan Wesley Zheng[1,2]* and Jim Yang Lee[1]*

[1]Department of Chemical and Biomolecular Engineering, National University of Singapore, 10 Kent Ridge Crescent, Singapore 119260, Singapore. [2]Institute of Materials Research and Engineering (IMRE), A*STAR (Agency for Science, Technology and Research), 2 Fusionopolis Way, Innovis, #08-03, Singapore 138634.

Corresponding addresses: cheleejy@ nus.edu.sg; wesley-zheng@imre.a-star.edu.sg

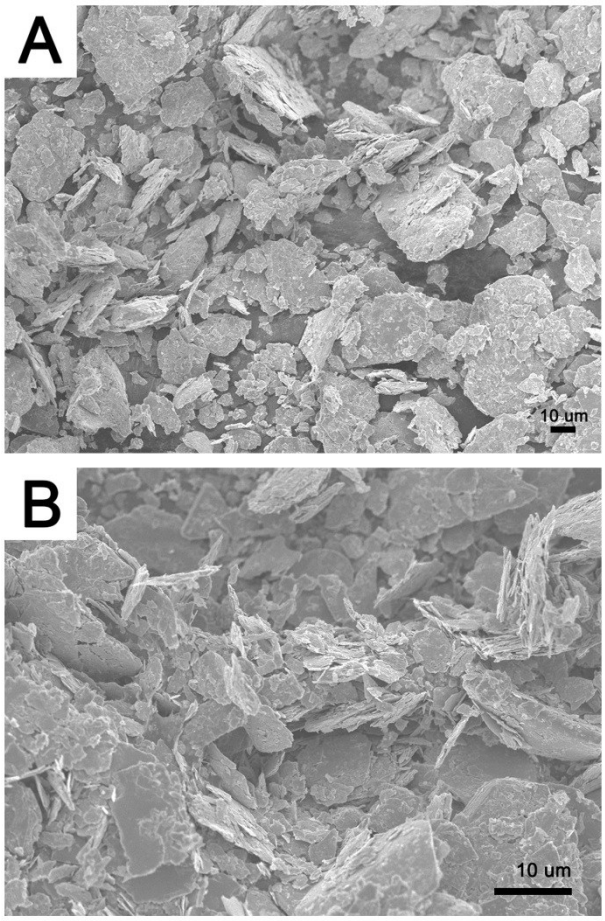

Fig. S1 (A and B) FESEM images of commercial MoS_2 particles.

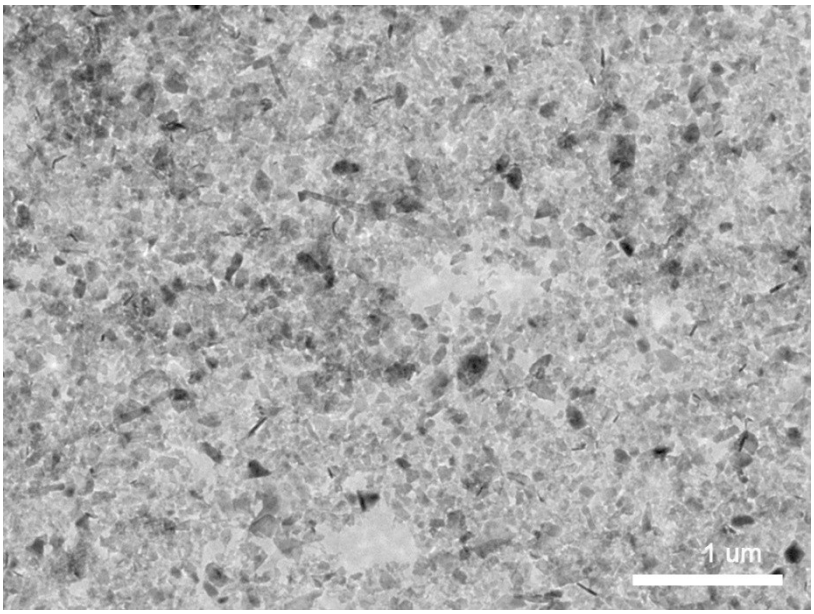

Fig. S2 TEM images of as-synthesized MoS_2 nanoflakes.

Table S1 Elemental compositions of MoS_2/GO treated at different temperature and reaction time.

	As-synthesized	600 ^oC for 3 h	600 ^oC for 6 h	700 ^oC for 3 h
Mo (%)	33.2	35.1	37.7	47.9
S (%)	65.4	60.5	56.1	20.5
O (%)	1.4	4.4	6.2	31.6

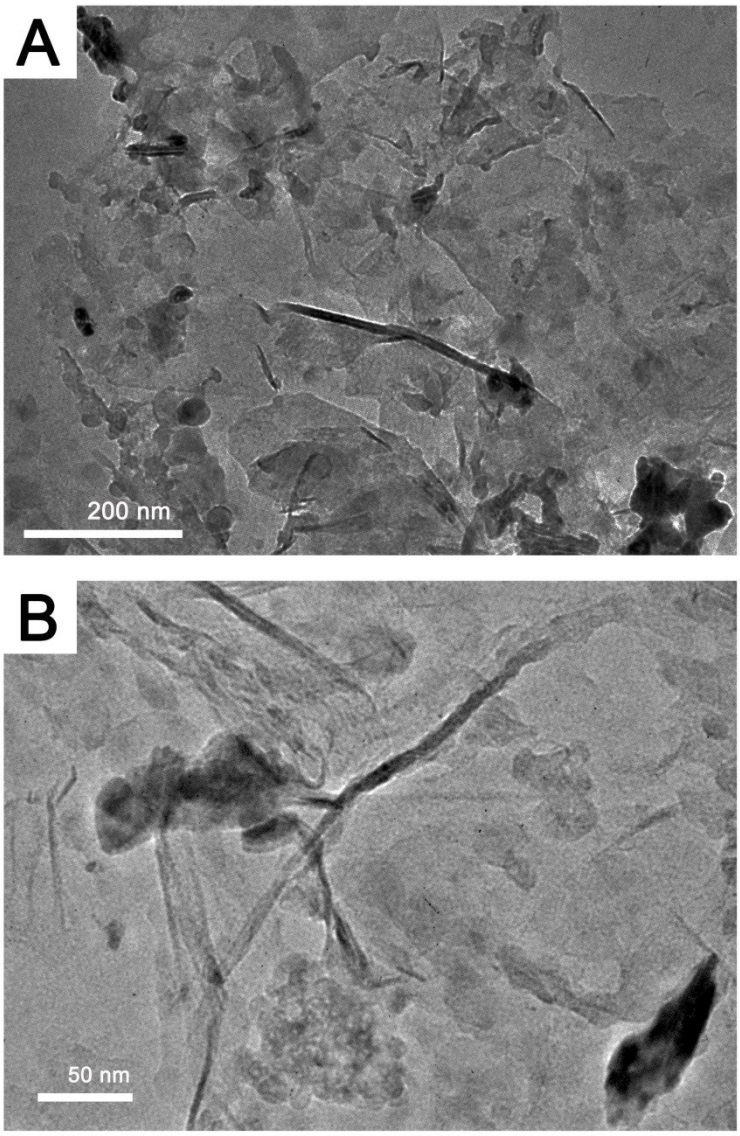

Fig. S3 TEM images of MoS_2/GO composite after heating at 700 ^oC for 3 hours.

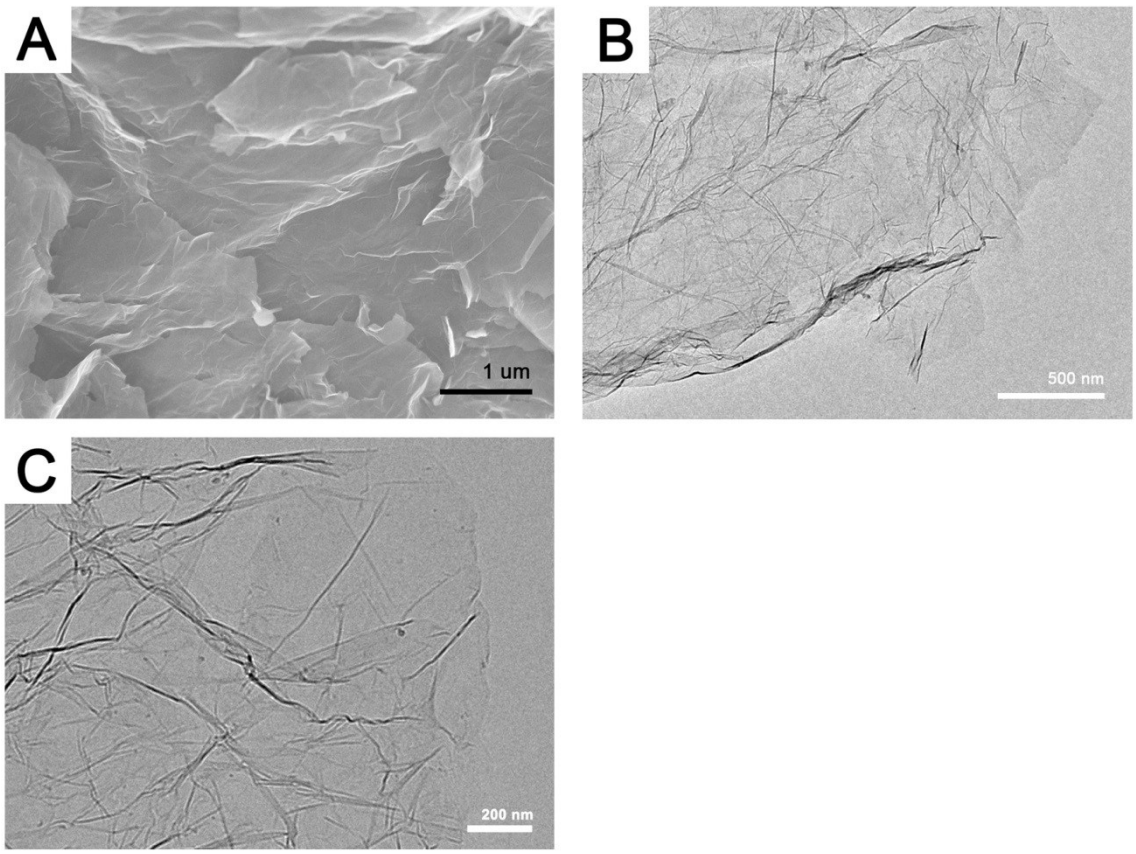

Fig. S4 (A) FESEM image and (B and C) TEM images of rGO synthesized from GO at 600 ^{o}C for 6 hours.

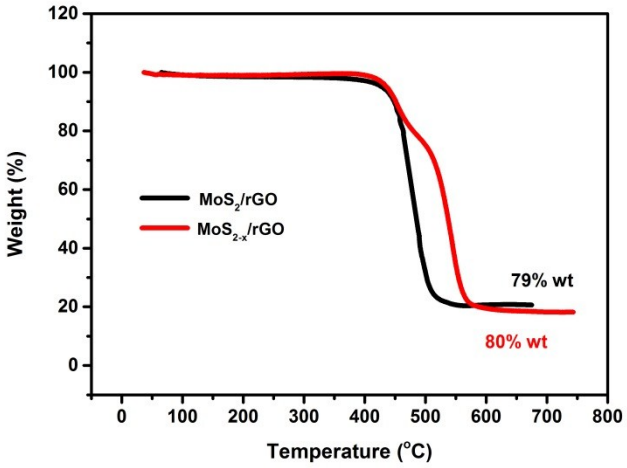

Fig. S5 TGA profiles of MoS_2/rGO and MoS_{2-x}/rGO in air (the final product was MoO_3).

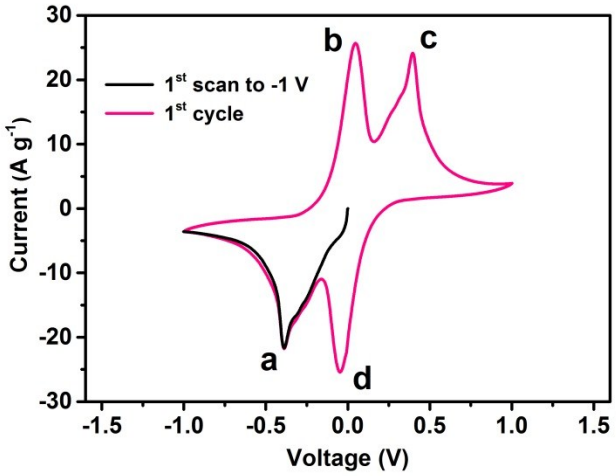

Peak a

Reaction on working electrode: $S_6^{2-} + 10e^- + 12Li^+ \rightarrow 6Li_2S$

Reaction on counter electrode: $4S_6^{2-} - 8e^- \rightarrow 3S_8$

Peak b

Reaction on working electrode: $6Li_2S - 10e^- \rightarrow S_6^{2-} + 12Li^+$

Reaction on counter electrode: $3S_8 + 8e^- \rightarrow 4S_6^{2-}$

Peak c

Reaction on working electrode: $4S_6^{2-} - 8e^- \rightarrow 3S_8$

Reaction on counter electrode: $S_6^{2-} + 10e^- + 12Li^+ \rightarrow 6Li_2S$

Peak d

Reaction on working electrode: $3S_8 + 8e^- \rightarrow 4S_6^{2-}$

Reaction on counter electrode: $6Li_2S - 10e^- \rightarrow S_6^{2-} + 12Li^+$

Fig. S6 Illustration of the electrode reactions for the redox peaks.

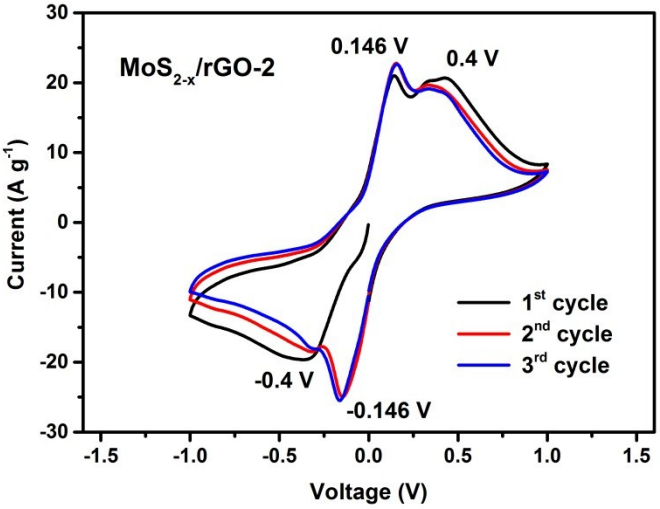

Fig. S7 Multi-cycle voltammograms of MoS_{2-x}/rGO-2 at 3 mV s^{-1}. (The MoS_{2-x}/rGO-2 composite was prepared as follows: MoS_2 nanoflakes were separated from the preparation solution by vacuum filtration, and heated at 600 ^oC in H_2 atmosphere for 6 hours. 0.04 g of the MoS_{2-x} formed as such was dispersed in 50 mL water, and mixed with 0.16 g rGO. The MoS_{2-x}/rGO-2 composite was then recovered by vacuum filtration.)

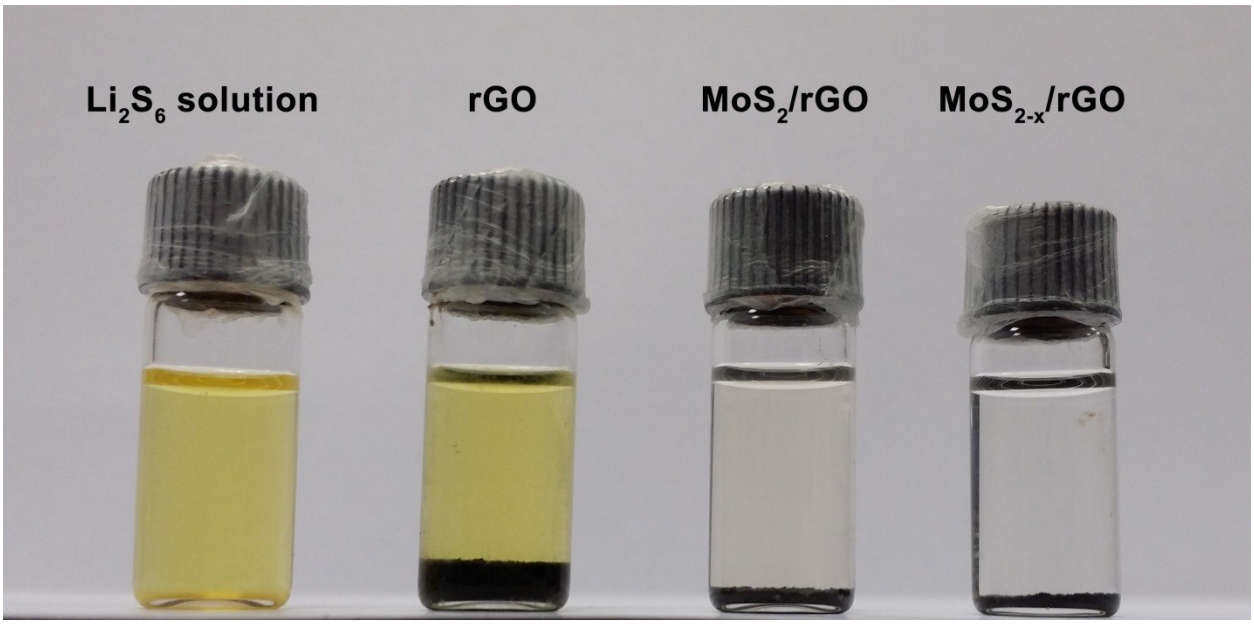

Fig. S8 Adsorption of Li_2S_6 solution (3 mmol L^{-1} in 1:1 (v/v) DME/DOL) on the same amount of rGO, MoS_2/rGO and MoS_{2-x}/rGO.

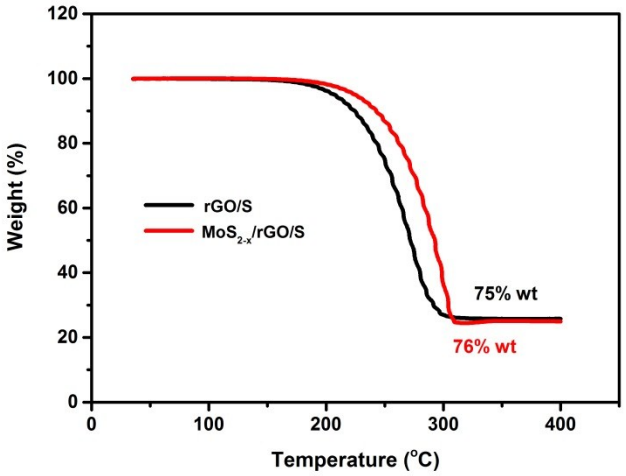

Fig. S9 TGA of rGO/S and MoS_{2-x}/rGO/S composites in N_2 (the final products were rGO for the rGO/S composite and MoS_{2-x}/rGO for the MoS_{2-x}/rGO/S composite).

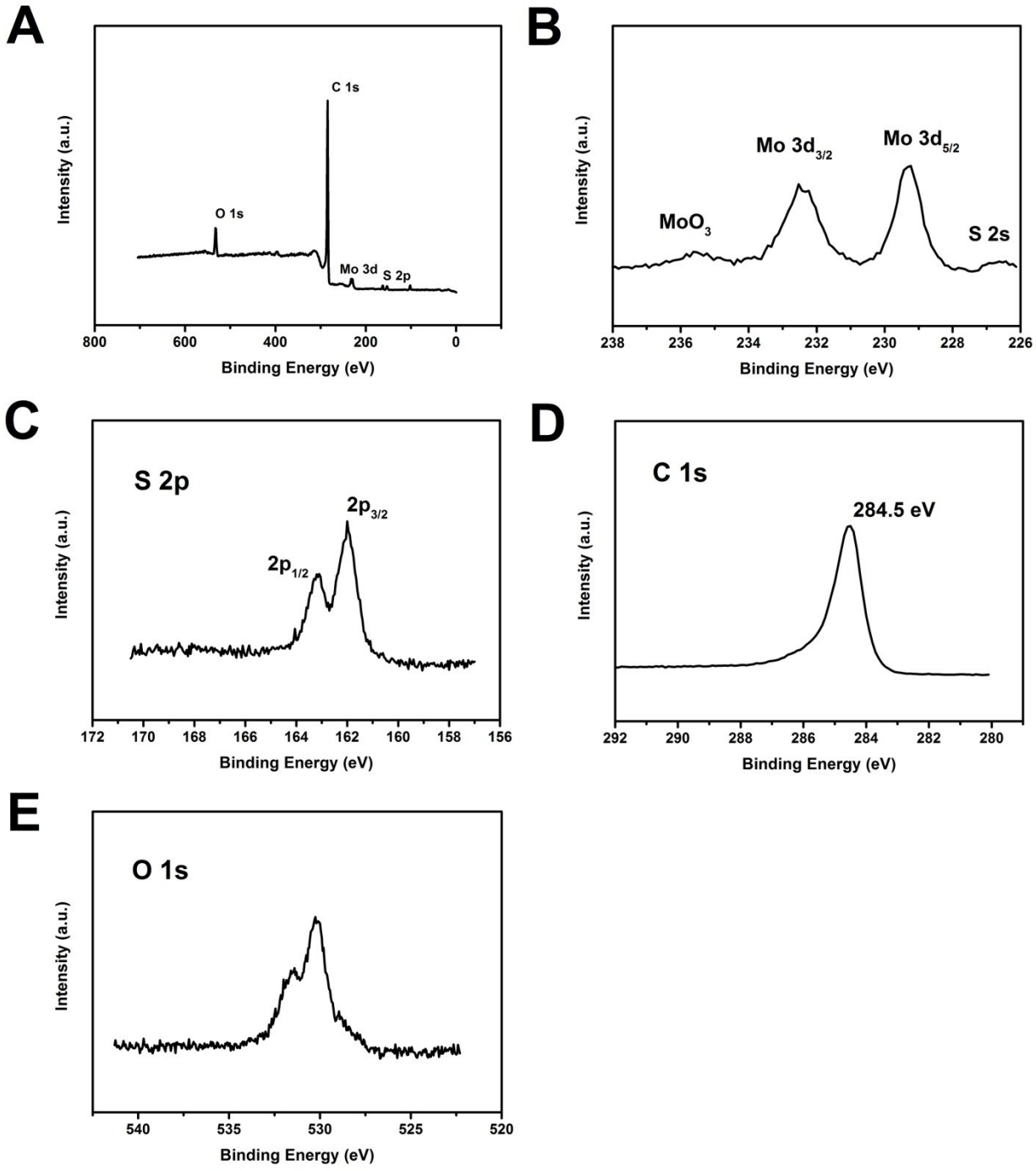

Fig. S10 (A) XPS survey scan, (B) Mo 3d, (C) S 2p, (D) C 1s and (E) O 1s X-ray diffraction patterns of MoS_{2-x}/rGO synthesized from MoS_2/GO at 600 ^oC for 6 hours.

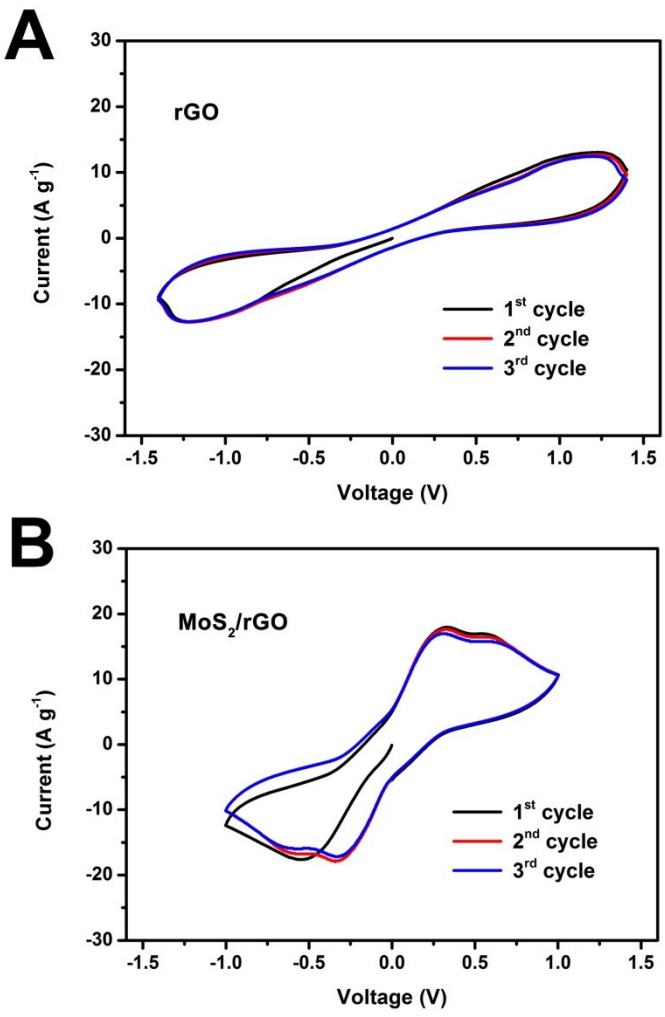

Fig. S11 Multi-cycle voltammograms of (A) rGO and (B) MoS_2/rGO at 3 mV s^{-1}.

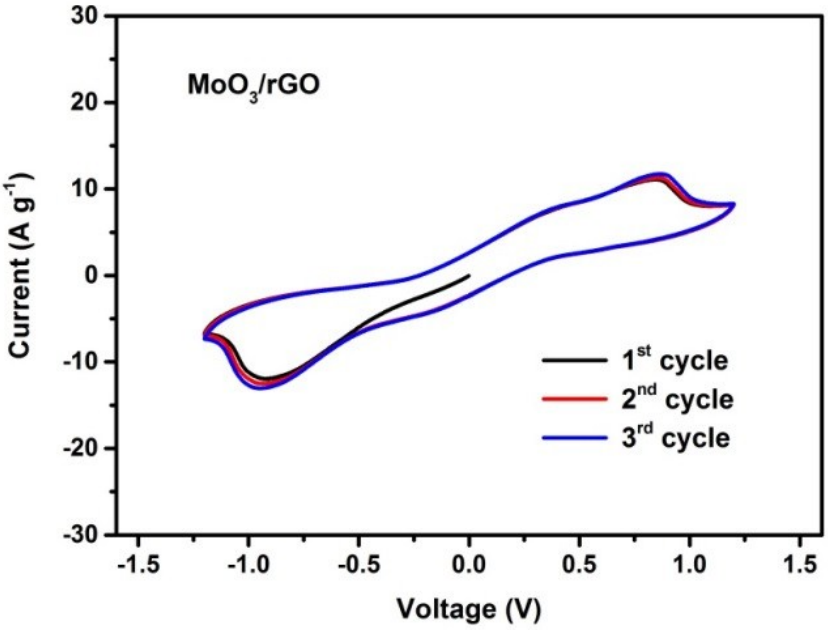

Fig. S12 Multi-cycle voltammograms of MoO_3/rGO at 3 mV s^{-1}. (The large polarization suggests that MoO_3 would have little effect on the measured electrochemical performance.)

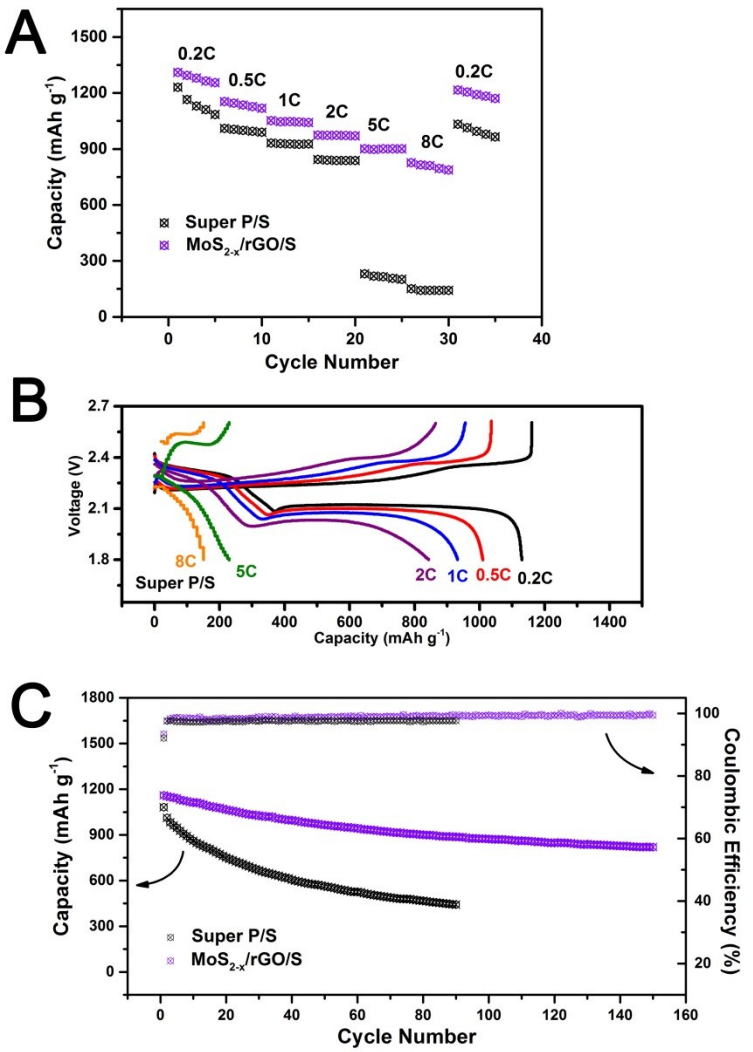

Fig. S13 (A) Comparison of rate performance at different C-rates, (B) galvanostatic discharge-charge curves and (C) cycle stability of Super P/S and MoS_{2-x}/rGO/S cells in the 1.8-2.6 V voltage range at 0.5 C. (The Super P/S composite was prepared by mixing sulfur power and Super P carbon in a 75:25 mass ratio and then sealed in a vial with Ar. The mixture was then heated at 155 ^{o}C for 5 hours. The Super P/S electrode was prepared by casting the NMP slurry containing Super P/S, PVDF and Super P in the weight ratio of 80:10:10 onto an Al foil.)

Table S2 Comparison of catalysts reported to date for lithium-sulfur batteries (All capacities are based on the mass of sulfur only).

Catalyst	Rate performance	Initial capacity	Cycling performance	Coulombic efficiency	Reference
Cobalt metal in the N-doped graphitic carbon	565 mAh g^{-1} (5 C)	1440 mAh g^{-1} (0.2 C)	850 mAh g^{-1} after 200 cycles	close to 100%	1
Platinum on graphene	1100 mAh g^{-1} (0.2 C)	1100 mAh g^{-1} (0.2 C)	789 mAh g^{-1} after 100 cycles	99.3%	2
TiN/C	411 mAh g^{-1} (5 C)	1069 mAh g^{-1} (0.2 C)	748 mAh g^{-1} after 50 cycles	N.A.	3
WS_2	380 mAh g^{-1} (1 C)	596 mAh g^{-1} (0.5 C)	542 mAh g^{-1} after 360 cycles	99%	4
RuO_2	912 mAh g^{-1} (0.5C)	912 mAh g^{-1} (0.5C)	513.3 mAh g^{-1} after 400 cycles	92.5%	5
MoS_{2-x}/rGO	826.5 mAh g^{-1} (8 C)	1159.9 mAh g^{-1} (0.5 C)	628.2 mAh g^{-1} after 500 cycles	99.6%	this work

Table S3 Comparison of MoS_{2-x}/rGO/S cathode to other cathodes of lithium-sulfur batteries reported to date.

Cathode	Rate performance	Initial capacity	Cycling performance	Reference
NG/S-20 TiO_2	833 mAh g^{-1} (4 C)	1102 mAh g^{-1} (1 C)	918.3 mAh g^{-1} after 500 cycles	6
MCM/Nb_2O_5/S	887 mAh g^{-1} (5 C)	1289 mAh g^{-1} (0.5 C)	913 mAh g^{-1} after 200 cycles	7
N-ACNT/G	770 mAh g^{-1} (5 C)	1152 mAh g^{-1} (1 C)	880 mAh g^{-1} after 80 cycles	8
S/(G-GCNs)	765 mAh g^{-1} (5 C)	1375 mAh g^{-1} (0.1 C)	943 mAh g^{-1} after 200 cycles	9
CNR-S	663 mAh g^{-1} (10 C)	1255 mAh g^{-1} (0.5 C)	1147 mAh g^{-1} after 500 cycles	10
S-HMT@CNT	888 mAh g^{-1} (7 C)	1113 mAh g^{-1} (1 C)	1040 mAh g^{-1} after 100 cycles	11
HPCR-805	646 mAh g^{-1} (5 C)	970 mAh g^{-1} (1 C)	700 mAh g^{-1} after 300 cycles	12
Sulfur nanodots on Ni foam	521 mAh g^{-1} (10 C)	1135 mAh g^{-1} (0.5 C)	895 mAh g^{-1} after 300 cycles	13
Vertically aligned S-G nanowalls	410 mAh g^{-1} (8 C)	~1000 mAh g^{-1} (0.15 C)	1220 mAh g^{-1} after 120 cycles	14
MoS_{2-x}/rGO/S	826.5 mAh g^{-1} (8 C)	1159.9 mAh g^{-1} (0.5 C)	628.2 mAh g^{-1} after 500 cycles	this work

References

1. Y.-J. Li, J.-M. Fan, M.-S. Zheng and Q.-F. Dong, *Energy Environ. Sci.*, 2016, **9**, 1998-2004.
2. H. Al Salem, G. Babu, C. V. Rao and L. M. Arava, *J. Am. Chem. Soc.*, 2015, **137**, 11542-11545.
3. T.-G. Jeong, D. S. Choi, H. Song, J. Choi, S.-A. Park, S. H. Oh, H. Kim, Y. Jung and Y.-T. Kim, *ACS Energy Lett.*, 2017, **2**, 327-333.
4. G. Babu, N. Masurkar, H. Al Salem and L. M. Arava, *J. Am. Chem. Soc.*, 2017, **139**, 171-178.
5. N. Ding, L. Zhou, C. Zhou, D. Geng, J. Yang, S. W. Chien, Z. Liu, M. F. Ng, A. Yu, T. S. Hor, M. B. Sullivan and Y. Zong, *Sci. Rep.*, 2016, **6**, 33154.
6. M. Yu, J. Ma, H. Song, A. Wang, F. Tian, Y. Wang, H. Qiu and R. Wang, *Energy Environ. Sci.*, 2016, **9**, 1495-1503.
7. Y. Tao, Y. Wei, Y. Liu, J. Wang, W. Qiao, L. Ling and D. Long, *Energy Environ. Sci.*, 2016, **9**, 3230-3239.
8. C. Tang, Q. Zhang, M. Q. Zhao, J. Q. Huang, X. B. Cheng, G. L. Tian, H. J. Peng and F. Wei, *Adv. Mater.*, 2014, **26**, 6100-6105.
9. J. Zhang, C. P. Yang, Y. X. Yin, L. J. Wan and Y. G. Guo, *Adv. Mater.*, 2016, **28**, 9539-9544.
10. S. Chen, X. Huang, H. Liu, B. Sun, W. Yeoh, K. Li, J. Zhang and G. Wang, *Adv. Energy Mater.*, 2014, **4**, 1301761.
11. J.-Y. Hwang, H. M. Kim, S.-K. Lee, J.-H. Lee, A. Abouimrane, M. A. Khaleel, I. Belharouak, A. Manthiram and Y.-K. Sun, *Adv. Energy Mater.*, 2016, **6**, 1501480.
12. Z. Zheng, H. Guo, F. Pei, X. Zhang, X. Chen, X. Fang, T. Wang and N. Zheng, *Adv. Funct. Mater.*, 2016, **26**, 8952-8959.
13. Q. Zhao, X. Hu, K. Zhang, N. Zhang, Y. Hu and J. Chen, *Nano Lett.*, 2015, **15**, 721-726.
14. B. Li, S. Li, J. Liu, B. Wang and S. Yang, *Nano Lett.*, 2015, **15**, 3073-3079.